Spectral and Anisotropic Corrections for GMS Satellite Data

Fang Xianjin (方先金)
Institute of Geophysics and Meteorology, University of Cologne, F. R. Germany
Received October 7, 1991

ABSTRACT

Using the radiative transfer simulation, the sampling study about the spectral and anisotropic corrections for GMS satellite data is carried out. The conversion factor and the anisotropic reflectance factor in inversion process of broadband radiation fluxes have been obtained for various underlying surface scenes in clear sky and for the case of overcast sky. The results demonstrate that the consideration of spectral and anisotropic corrections is essential for the earth radiation budget research using satellite data. The mean conversion factors for GMS are between 2.54 and 5.30. The values of the conversion factor are different for various observation angles, especially in cases of ocean, vegetation cover and wet soil surface. The error of retrieving broadband radiance without considering the difference of observation geometry is about 5.5%–15% for ocean, 4.5%–10% for various land surfaces. The calculated anisotropic factors for ocean and cloud scenes are in good agreement with those estimated from Nimbus–7. For Land, desert and snow scenes, the calculated values in backward scattering direction are smaller than the measured.

1. INTRODUCTION

Recent progress in climate research enhances the demand for accurate energy exchange between climatic system and space, which is given by earth radiation budget at the top of the atmosphere. Earth radiation budget as a tractor of climate change and forcing function is a key component of the climate monitoring system and effects further climate change. The climate modelling about the impact simulation of trace gases such as CO_2, CH_4 and CFCs on climate change has revealed that these gases affect the earth surface temperature through changing of the earth radiation budget. In turn,the long–term variation of earth radiation budget at the top of the atmosphere and at the earth surface will give a direct estimate of the change in the climate forcing due to desertification and deforestation, change in aerosols and trace gases, and change in cryosphere. Therefore, one of major objectives of ISCCP (International Satellite Cloud Climatology Project) in WCRP (World Climate Research Program) is to determine earth radiation budget.

For determining the earth radiation budget with available spatial resolution, satellite data have been commonly used in recent studies. However meteorological satellites (such as NOAA, METEOSAT, GMS and FENGYUN) measure only in narrowband and in narrow field of view. But in the calculation of earth radiation budget and in practical application for climate research, we need to know the broadband radiation fluxes. Therefore there is a considerable disagreement between possible data use and the objective in radiation budget research. In this regard the problem in the shortwave portion of the spectrum is more difficult than the longwave portion due to complexity of shortwave spectral property.

The radiance measured by satellite depends on the status of atmosphere, measurement geometry and property of the underlying surface. To infer the broadband radiation flux from a single observation made at the top of the atomsphere by a narrowband sensing instrument,

the conversion factor which must be applied to the filtered radiance to derive the broadband radiance, the angular distribution of the reflected energy to get hemispheric reflectance, the optical state and properties of intervening atmosphere to correct for its masking effect have to be known. The common difficulties in broadband radiation flux computations from satellite data are large variability in reflected radiation field and spectral correction of scanning radiometer measurement in the intensity of one viewing angle.

Within this paper, the spectral and angular corrections of satellite data are investigated with a simpling study for GMS measurement in narrowband and in single angle of view. As mentioned above, the measurement from GMS satellite in solar range requires a correction to get broadband radiation fluxes. For this propose, the values of the spectral conversion factor and anisotropic reflectance factor have been calculated with a radiative transfer modelling. The uncertainties of two correction factors about the changes of sun and satellite angle and underlying surface property have been revealed. This study will probably lead to achieve the correction dataset in inversion process from GMS narrowband measurement to broadband radiation fluxes for satellite use. The practical application of this dataset in earth radiation budget research is subject of forthcoming papers.

II. THEORETICAL MODEL DESCRIPTION

The broadband radiation flux can be estimated by definition of the anisotropic reflectance factor (or called as bidirectional reflectivity factor) and the spectral conversion factor from Eq. (1)

$$M(\theta_0,S)=\frac{\pi F_{\mathrm{sol}}(\theta_0,\theta,\psi,S,)L_{\mathrm{sat}}(\theta_0,\theta,\psi,S,)}{R(\theta_0,\theta,\psi,S,)}. \tag{1}$$

where θ_0: solar zenith angle; θ:observation zenith angle; ψ: azimuth angle, with forward scattering $\psi=0$; S: scene; M: reflected solar radiation flux at atmosphere top; L_{sat}: radiance measured by satellite; F_{sol}: conversion factor from narrowband to broadband radiances; R: anisotropic reflectance factor.

Therefore, the derivation of broadband radiation flux from narrowband measurement involves two computational steps: the spectral and angular corrections. The spectral correction is to determine the conversion factor from filtered radiance measured by satellite to unfiltered radiance, and it depends on satellite sensor. The angular correction is to consider the angular distribution of reflected radiance and to convert unfiltered radiance to radiation flux. On the other hand, in order to determine the conversion factor and the anisotropic reflectance factor in Eq. (1), it is necessary to calculate the unfiltered and filtered radiances, because the broadband radiation flux can also be obtained from the unfiltered radiation $L_{\mathrm{sol}}(\theta_0,\theta,\psi)$ by Eq.(2)

$$M(\theta_0,S)=\int_0^{\pi/2}\int_o^{2\pi}L_{\mathrm{sol}}(\theta_0,\theta,\psi,S)\sin\theta\cos\theta d\theta d\psi, \tag{2}$$

and the conversion factor is the ratio of the unfiltered to filtered radiances.

In this work the calculation procedures for unfiltered and filtered radiances are based on theoretical radiative transfer calculations which have been described in detail by Raschke (1971, 1972). In this theory, the equation of radiative transfer for monochromatic radiation within a plane–parallel and horizontally homogeneous atmosphere is resoluted. The basic concept is to expend upward and downward radiances into an even Fourier series.

$$L_j(\theta,\psi,\delta) = \sum_{k=0}^{N} L_j^k(\theta,\delta).\cos(K(\psi-\psi_0)), \tag{3}$$

where ψ_0 :solar azimuth; δ: optical depth of the atmosphere; L_j^k : K–th Fourier coefficient for radiances; i = 1 for upward radiance; i = 2 downward radiance.

At the same time, the scattering phase function is expanded into a series of Legendre polynomials:

$$P(\Theta_s) = \sum_{j=0}^{N} W_j P_j(\cos\Theta_s), \tag{4}$$

where Θ_s: the scattering angle; $P(\Theta_s)$: scattering phase function; W_j: j –th Legendre coefficient; $P_j(\cos\Theta_s)$: j –th Legendre polynomial with argument Θ_s.

For scene of cloud,the droplet size distribution of altostratus is taken from Hansen (1971):

$$n(r) = r^{(1-3V_{\text{eff}})/V_{\text{eff}}} \cdot \exp(-\bar{r}/r_{\text{eff}} V_{\text{eff}}), \tag{5}$$

where: $n(r)$ is the number density; $\bar{r}_{\text{eff}}$ is the mean effective radius (7.01 μm); V_{eff} is the effective variance (0.113). In the case of cloud, the cloud droplets have a strong forward scattering characteristic which would require a large number of Legendre terms to represent this forward peak. For reduction of the number the Delta function approximation (Potter, 1970) is used. The cloud altitude is located as the cloud top at 4 km and the cloud is defined to be 1 km thick with an optical thickness of 60.

The method of radiative transfer solution is by iteration (Raschke, 1971). In this model, multiple scattering has been in detail considered. The model calculation in this work is until to the height of 70 km. In 87 spectral intervals the monochromatic radiative transfer equation in solar spectral range (0.2–3.58μm) is solved in order to describe the atmospheric and the surface properties. In the calculation the absorption by water vapour, carbon dioxide and aerosols is formulated according to Kerschgens (1978). For aerosol scattering the following particles (taken from Shettle and Fenn, 1975): stratospheric, tropospheric, and boundary layer aerosols are used. The discrimination between rural and maritime–type aerosols is considered. The aerosol scattering phase function is calculated for spherical particles (Quenzel and Müller, 1978). The molecular scattering, which just exhibits Rayleigh–type scattering, is described by the Rayleigh phase function. The main input data and description can be found in detail from kerschgens (1978), Stuhlmann and Raschke (1987).

The conversion factor and the anisotropic reflectance factor depend on the observed "scene" besides on the satellite viewing geometry from Eq. (1). "Scene" is a parameter being capable of variation in the measurement place on the earth and in status of the atmosphere. The scene is not only changed with the geographic position but also with time. The atmospheric and underlying covered characters in different seasons may be different at one site. By the modelling calculation, it must be determined in which scene the conversion factor and angular reflectance factor have considerable variations and in which scene their variations are not so large and can be neglected. This sensitivity study should first be carried on for ocean, land, desert and snow underlying surface scenes. Because this kind of study takes much computing time, the sensitivity study can not be made for the atmospheric status at every site and every time and only made for standard atmosphere model.

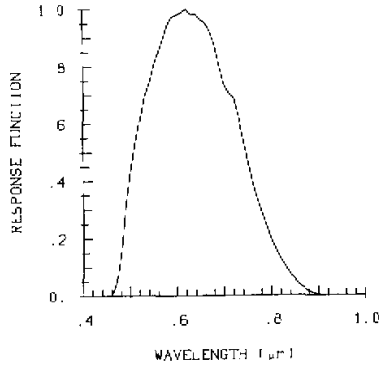

Fig.1. Spectral filter function for GMS-3 visible channel.

III. CONVERSION FACTOR FOR THE GMS-3 VISIBLE CHANNEL

The retrieval of unfiltered broadband (0.2–3.58μm) radiance $L_{sol}(\theta_0,\theta,\psi)$ from filtered radiances $L_{sat}(\theta_0,\theta,\psi)$ in narrow band measured by satellite visible channel requires the knowledge of the appropriate conversion factor F_{sol} . Previous theoretical research on METEOSAT conversion factor has been made (Kriebel, 1983; Wiegner, 1985; Stuhlmann and Raschke, 1987). Using a more extensive theoretical approach, they analyzed variability of the conversion factor between unfiltered and filtered radiances over a large set of sunface reflectance, atmospheric state and relative observational geometry. Their results showed that the variation of the conversion factor for METEOSAT over a surface could reach ± 1 around average values 2.8 and 2.4 for vegetation and bare surface respectively. Obviously, the results of these analyses can not be directly extended to other satellites, because of F_{sol} depending on the spectral reponse of the satellite sensor.

Based on conversion factor F_{sol} , it is assumed as

$$L_{sol}(\theta_0,\theta,\psi,S) = F_{sol}(\theta_0,\theta,\psi,S)L_{sat}(\theta_0,\theta,\psi,S) \tag{6}$$

with

$$L_{sat}(\theta_0,\theta,\psi,S) = \int_{0.4\mu m}^{1.1\mu m} L_\lambda^t(\theta_0,\theta,\psi,S)\varphi_{sat}\,d\lambda, \tag{7}$$

$$L_{sol}(\theta_0,\theta,\psi,S) = \int_{0.20\mu m}^{3.58\mu m} L_\lambda^t(\theta_0,\theta,\psi,S)d\lambda, \tag{8}$$

where $L_\lambda^t(\theta_0,\theta,\psi,S)$ is the spectral radiance leaving the top of the atmosphere, and φ_{sat} is the spectral response of the satellite shortwave channel. In the study the GMS-3 spectral responses have been chosen. The filter function value of GMS-3 φ_{sat} is show in Fig. 1.

The spectral radiance leaving the top of the atmosphere L_λ^t can be calculated for multiple scattering within a plane parallel and horizontally homgeneous atmosphere described above. Based on the calculation and the analysis for the METEOSAT and ERBE spectral responses by Wiegner (1985) and Stuhlmann and Raschke (1987), the conversion factors for ocean, land, desert and snow schemes are mainly dependent on the solar zenith angle existing and it is little dependent on observational angles θ and ψ. These dependences can be explained from definition of the conversion factor and the fact that the anisotropies of filtered and unfiltered radiance have not essential difference (Wiegner, 1985). Therefore, the conversion

factor $F_{sol}(\theta_0,\theta,\psi,S)$ can be expressed as:

$$F_{sol}(\theta_0,\theta,\psi,S)=\bar{F}_{sol}(\theta_0,S).F'_{sol}(\theta_0,\theta,\psi,S) \tag{9}$$

whit

$$\bar{F}_{sol}(\theta_0,S)=\frac{\int_\Omega L_{sol}(\theta_0,\theta,\psi,S)d\Omega}{\int_\Omega L_{sat}(\theta_0,\theta,\psi,S)d\Omega}, \tag{10}$$

$$F'_{sol}(\theta_0,\theta,\psi,S)=\frac{L_{sol}(\theta_0,\theta,\psi,S)\int_\Omega L_{sat}(\theta_0,\theta,\psi,S)d\Omega}{L_{sat}(\theta_0,\theta,\psi,S)\int_\Omega L_{sol}(\theta_0,\theta,\psi,S)d\Omega}, \tag{11}$$

here

$$d\Omega=\sin\theta\cos\theta d\theta d\psi. \tag{12}$$

$\bar{F}_{sol}$ is the mean conversion factor, i. e., the ratio of the unfiltered isotropic radiance to the filtered and F'_{sol} indicates the deviation of anisotropic to isotropic conversion factor. For first approximation F'_{sol} is 1. In order to save computation time, $\bar{F}_{sol}$ is calculated with two stream approximation (Kerschgens et al., 1978) in which the same input data of atmosphere and surface properties are used.

Fig. 2 illustrates the mean conversion factor $\bar{F}_{sol}$ depending on solar zenith angle for various underlying surface scenes in clear sky and for the cloud case. The values of $\bar{F}_{sol}$ are first changing with spectral distribution of the underlying reflected radiation. Therefore, considerable differences exist for different scenes. The values of mean conversion factor $\bar{F}_{sol}$ are between minimum of 2.54 for snow to maximum of 5.30 for forest when $\theta_0=0°$. The difference of mean conversion factor for different scenes becomes especially greater when the sun's ray comes from zenith direction (θ_0 is small). The difference decreases with increasing θ_0 . The dependence on solar zenith angle is important for the scenes of forest, wet soil, but insignificant for desolate land, desert, snow and cloud. The influence of atmospheric status can be considered with various standard atmosphere models and different aerosol loading and boundary layer condition.

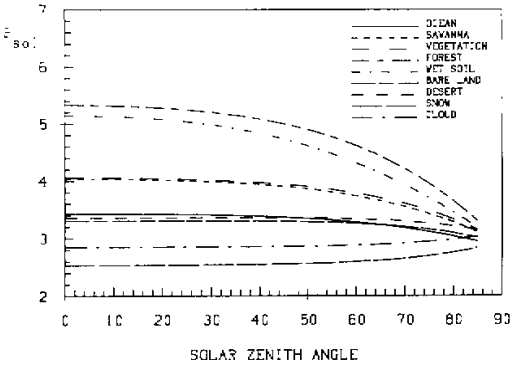

Fig.2. Mean conversion factor $\bar{F}_{sol}$ changing with sun zenith angle.

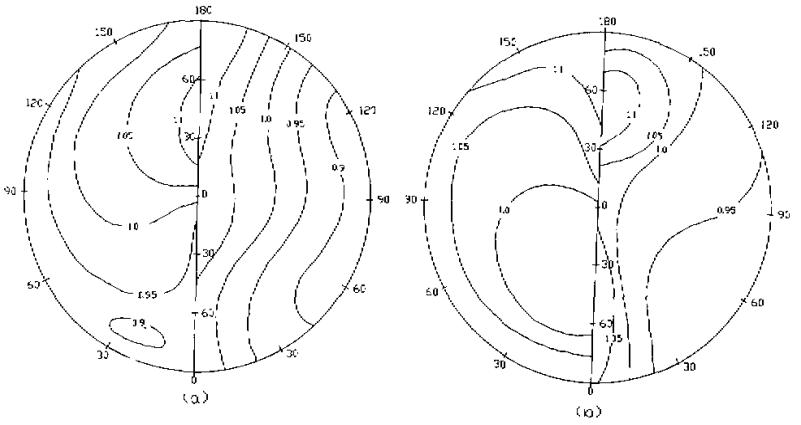

Fig.3. Distributions of the conversion factor F'_{sol} as function of observation geometry (θ,ψ) for different scenes in clear sky and different solar zenith angles (a) the left for ocean, $\theta_0 = 37.5°$ the right for vegetation, $\theta_0 = 77.5°$ (b) the left for snow, $\theta_0 = 17.5°$ the right for desert, $\theta_0 = 57.5°$.

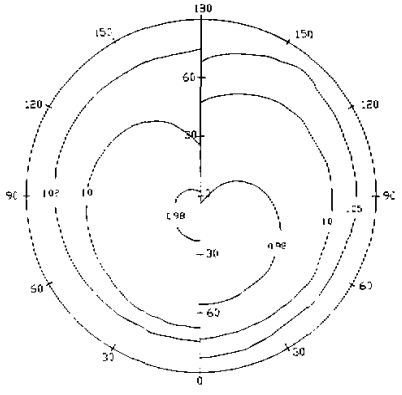

Fig.4. Distributions of the conversion factor F'_{sol} as function of observation geometry (θ,ψ) for cloud scene. the left is for $\theta_0 = 37.5°$ and the right is for $\theta_0 = 77.5°$.

The values of F'_{sol} which are dependent on the observed angle have been calculated and given for different scenes and four values of solar zenith angles as examples shown in Figs. 3 and 4. Fig. 3 gives the distribution of F'_{sol} as function of observation geometry (θ,ψ) for different underlying surface scenes in clear sky and Fig. 4 gives the distribution of F'_{sol} for cloud scene in two cases of solar zenith angle. In these figures, the pole of the projection is the viewing zenith angle $\theta = 0°$. The zenith angle θ increases radially outward from the pole on a linear scale. The azimuth $\psi = 0°$ respresents the forward scattering direction and $\psi = 180°$ respresents the backward scattering direction.

The isopleth of $F'_{sol} = 1$ in these figures represents the case of isotropic radiance. The deviation from the value of 1 indicates anisotropic character. The larger is the deviation, the

greater is the error estimated from the mean conversion factor $\bar{F}_{sol}$. For ocean case of $\theta_0 = 37.5°$, the maximum of F'_{sol} larger than 1.1 occurs in the backward scattering when satellite viewing zenith angle is between 20° and 60°, e.g., the error of the retrieving broadband radiance due to using $\bar{F}_{sol}$ instead of F_{sol} is about 10%, and the values calculated are on the low side. The minimum of F'_{sol} smaller than 0.9 occurs when $\theta > 65°$ and $\psi < 35°$. Thus, the broadband radiance derived from $\bar{F}_{sol}$ is about 10% larger than that retrieved with F_{sol}. From the distribution of F'_{sol} for case of ocean, the values in backward scattering are larger than those in forward scattering direction. For land scene with vegetation cover ($\theta_0 = 77.5°$), the values of F'_{sol} are between the minimum 0.9 and the maximum 1.1 and mainly dependent on viewing zenith angle θ. The values increase with increasing θ. For case of snow scene ($\theta_0 = 17.5°$), the values of F'_{sol} are larger in backward scattering when $\theta > 60°$ and $\psi > 120°$, and smaller when of $\psi < 90°$. $\theta < 60°$. For desert scene of $\theta_0 = 57.5°$, the values of F'_{sol} in backward and forward scattering are larger than 1 and are smaller than 1 in the range of $20° < \psi < 150°$ with larger θ. The values in this case decrease with increasing θ. In Fig.4, the distributions of F'_{sol} for cloud scene are quite simple, the values of F'_{sol} increase basically with increasing θ. But deviation of the conversion factor is between +/−3% for solar zenith angle $\theta_0 = 37.5°$ and +/−7% for $\theta_0 = 77.5°$.

From Eqs. (1) and (9), if the value of F'_{sol} is not approaching to 1, the error in the case that the effect of observation geometry has been not considered in retrieving process of broadband radiance would become larger. This kind of error can be explained with mean relative difference which be calculated from equation (13)

$$\frac{\Delta F_{sol}}{\bar{F}_{sol}} = \sum_{i}^{N} \left| \frac{F^i_{sol} - \bar{F}^i_{sol}}{\bar{F}^i_{sol}} \right| = \sum_{i}^{N} \left| F'^i_{sol} - 1 \right| . \tag{13}$$

Table 1. The Mean Relative Differences of $\Delta F_{sol} / \bar{F}_{sol}$

scene	mean relative difference (%)			
	$\theta_0 = 17.5°$	$\theta_0 = 37.5°$	$\theta_0 = 57.5°$	$\theta_0 = 77.5°$
ocean	5.6	6.5	9.3	14.7
savanna	7.7	7.8	8.0	8.5
vegetation	7.3	7.6	9.1	9.7
forest	7.6	7.5	8.9	9.9
wet soil	6.5	7.3	8.7	9.4
bare land	4.9	5.6	7.0	7.8
desert	3.9	5.5	6.2	6.5
snow	3.4	3.3	3.7	3.7
cloud	1.5	1.8	1.9	3.7

In Table 1 the mean relative differences for various scenes and for four cases of solar zenith angle are shown. The maximal mean relative difference occurs in scene of ocean for $\theta_0 = 77.5°$. The minimum occurs in scene of cloud for $\theta_0 = 17.5°$. The mean relative difference increases with increasing solar zenith angle for all scenes. The variations of mean relative difference are about 5.5%–15% for ocean; 4.5%–10% for different land surfaces; 3.9%–6.5% for desert; 3.3%–3.7% for snow and 1.5%–3.7% for cloud. Therefore, in

retrieval model from narrowband to broadband radiance, the change of the conversion factor with observation geometry for ocean and land surfaces must be considered in model, in order to reduce the inversion error. For snow and cloud overcast scenes the change of conversion factor with observation geometry in smaller solar zenith angle can be neglected within an accuracy of 4%.

IV. ANGULAR ANISOTROPIC CORRECTION

The knowledge about the anisotropic reflection properties of observed medium is another prerequisite for inferring broadband flux quantities such as radiation flux and broadband planetary albedo from a single observation made by a narrow field of view instrument. To a large extent, the instantaneous accuracy of the estimated broadband flux is limited by the uncertainty in applying the angular dependence model.

The angular dependence function is generally described with the anisotropic reflectance factor. The anisotropic reflectance model has been developed in order to account for anisotropic reflectance properties. The anisotropic reflectance factor can be obtained from the same model as the spectral conversion factor. In addition , for climate scale the anisotropic reflectance factors have been restricted from the Nimbus–7 Earth Radiation Budget Experiment (ERBE) to eight uniform surface types (Taylor and Stowe, 1984). The anisotropic reflectance factor should be not dependent on radiometer filter function. Therefore, in order to obtain anisotropic reflectance factor which can be applied to any instrument measurement, the model calculation has to be made for unfiltered broadband condition. But because of obvious interaction between the atmosphere and various underlying surfaces and obvious spectral reflectance properties of the different underlying surfaces, the anisotropic factor is dependent on the pattern and properties of the underlying surface. Therefore, the anisotropic reflectance factor is expressed as

$$R(\theta_0,\theta,\psi,S)=\frac{DL_{\mathrm{sol}}(\theta_0,\theta,\psi,S)}{\int_0^{\pi/2}\int_o^{2\pi}L_{\mathrm{sol}}(\theta_0,\theta,\psi,S)\sin\theta\cos\theta d\theta d\psi} \tag{14}$$

with the normalized property

$$\frac{1}{\pi}\int_0^{\pi/2}\int_0^{2\pi}R(\theta_0,\theta,\psi,S)\sin\theta\cos\theta d\theta d\psi=1. \tag{15}$$

Here it is clearly shown that the radiance angular distribution at the top of the atmosphere should be derived for determination of the anisotropic reflectance factor.

The broadband radiance $L_{\mathrm{sol}}(\theta_0,\theta,\psi,S)$ has been obtained with Eq. (8) through integration of spectral radiance at the top of the atmosphere. In order to calculate $R(\theta_0,\theta,\psi,S)$ from Eq. (14), the zenith angle of observation and azimuth have been divided into 18 and 17 intervals, respectively, totally into 306 bins. The value of $R(\theta_0,\theta,\psi,S)$ in each of bins represents the average value and is constant within this bin. In Figs. 5 and 6 the values of $R(\theta_0,\theta,\psi,S)$ calculated and measured from Nimbus–7 are shown as examples.

Fig. 5(a) illustrates distributions of the anisotropic reflectance factors calculated (left) and derived by Nimbus–7 (right) for ocean surface. The calculation is made for midlatitude summer standard atmosphere. The spectral reflection on water surface has been treated according to Fresnel's Law. The aerosol distribution is taken as maritime standard model. The boundary layer visibility is taken as normal 23 km. The solar zenith angle is 57.5°. A marked characteristic in calculated results of the anisotropic reflectance factor R is that the value of R reaches its maximum along isoline of θ when azimuth is smaller than 15°. It means that

the forward scattering of the sun's beam for ocean–atmosphere system is larger than the scattering in other directions. The maximum reflected radiance is four times ($R=4$) larger than the isotropic radiance when zenith angle of viewing $\theta > 70°$ and azimuth $\psi < 15°$. The value of R increases with the increasing of θ. The minimum occurs when observational zenith angle is small. The characters of occurring extremes (the maximum and the minimum) can be found for other solar zenith angles. But the conspicuous extent of these characters is affected by the change with sun incident angle and it becomes more remarkable as the solar zenith angle increases.

The corresponding anisotropic reflectance factor measured from Nimbus–7 data is shown in the right of Fig. 5(a). The calculated values of $R$are in a good agreement with the measured. Both the calculated and the measured are increasing with the increasing of the viewing angle and show a strong forward scattering. But the measured values in backward scattering are greater than the calculated. The difference might be caused by different aerosol distribution between the model atmosphere and the real atmosphere. On the other hand, the modelling calculation is carried out for a certain solar zenith angle, while the value derived from Nimbus–7 is for an interval of solar zenith angle.

For land surface the calculated and the measured anisotropic reflectance is shown as another example in Fig. 5(b). The radiative transfer calculation is made for vegetation surface on which the simple Lambertian reflectivity is used, e. g., the radiation reflected in certain solar zenith angle is same in all observation directions. Aerosol distribution is considered as rural standard type. The standard atmosphere, boundary layer condition and solar zenith angle are as same as those in the left Fig. 5(a).

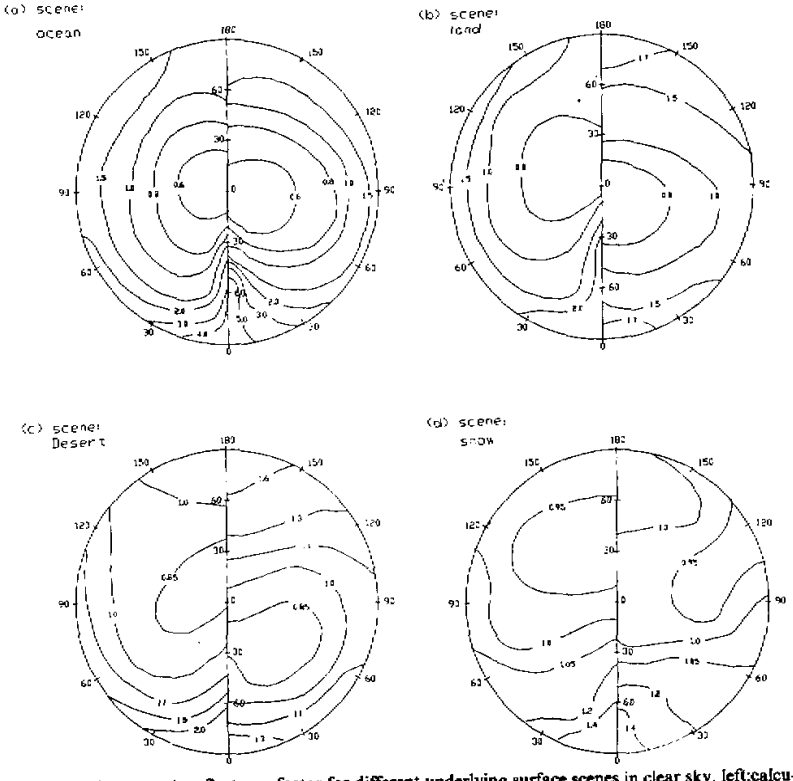

Fig. 5. Anisotropic reflectance factor for different underlying surface scenes in clear sky. left:calculated, $\theta_0 = 57.5°$ right: Nimbus–7 data, $53.1° \leqslant \theta_0 < 60.0°$.

For land scene the calculated value of R changes in a smaller range than that for ocean. The maximum of R is larger than 2.0 and occurs in the forward scattering direction when the viewing angle θ is larger than about 25° . The values of R in the backward scattering are smaller than those in the forward scattering. The measured value of R changes less slightly than the calculated, and the forward and backward scattering are not very different from each other. Comparing the measured with the calculated, the latter in forward scattering is larger than the former, but in backward scattering is smaller than the former. And both increase with the increasing of viewing zenith angle. The differences between the calculated and the measured anisotropic reflectance factors for land surface described above are found in the same manner for desert surface in Fig.5(c) and for snow scene in Fig.5(d).

The difference described above between values of the anisotropic reflectance factor calculated with radiative tranfer modelling and estimated from Nimbus–7 has also been found in Wiegner's work (1985). The differences are mainly caused by the assumption in the model, in which the surface reflection is regarded as isotropic. However, the real surface is usually an anisotropic reflecting surface. But the measured data for this kind of underlying surface are much insufficient to be applied for the earth radiation budget research. Wiegner (1985) collected limited anisotropic matrix data for sand surface from experiments in laboratory and took them as input to model. He found that the results were evidently improved and in an approximate agreement with the data from Nimbus–7. It means that the anisotropic distribution of the radiance at the top of atmosphere is sensitive to the anisotropic reflectivity on the surface in model input data.

For cloud scene, the values of anisotropic reflectance factor calculated and estimated from Nimbus–7 are shown as examples in Fig. 6. The calculated results are in a quite good agreement with measured values. The maximum with $R>1.5$ occurs in forward scattering with larger zenith angle of viewing. The minimum occurs when observation angle is smaller than 30° .The values of R increase with increasing zenith angle of viewing

From the analysis above, it can be found that the reflected radiance at the top of the atmosphere possesses strong anisotropy. The isotropic assumption in modelling of the earth radiation budget would lead to a large error which is variable for different scenes, viewing angles and azimuth. For ocean this error might be larger than those for land and desert surfaces. For cloud and snow scenes, this error is smaller than those for other scenes. Form Figs. 5 and 6, it is found that the error in isotropic earth radiation budget modelling increases with decreasing reflecting power of scenes. Therefore the anisotropic correction should be carried out in the earth radiation budget modelling, especially for ocean and vegetation cover surface. The anisotropic distribution in model is different from that measured in backward scattering direction when isotropic surface is taken as input. While the surface anisotropic data are directly introduced, the calculated results are improved. But because of much insufficient data for anisotropic surface and too much computing time taken by anisotropic calculation, the experimental anisotropic model derived from measured data can be, in general, used in the earth radiation budget research.

V. CONCLUSION AND REMARK

In order to derive broadband planetary albedo or broadband radiation fluxes at the top of the atmosphere from narrowband satellite data, the conversion factor and the anisotropic reflectance factor must be first known. With a theoretical calculation, the spectral and the anisotropic corrections for GMS–3 data have been specially carried out. From the analyses of the calculated results the spectral correction can be expressed with the conversion factor that

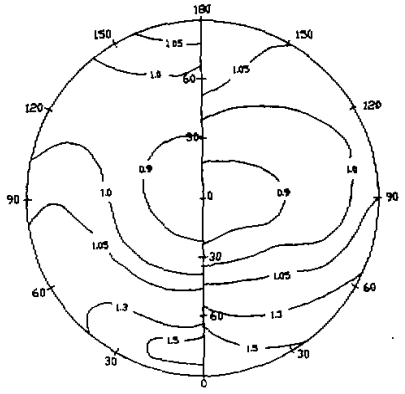

Fig.6. Anisotropic reflectance factor for cloud scene. The left is the value calculated for $\theta_0 = 57.5°$ and the right is the value estimated from Nimbus-7 for $53.1° \leqslant \theta_0 < 60.0°$.

is the ratio of the unfiltered to the filtered radiances integrated over spectrum. It is found that the conversion factor mainly depends on the solar zenith angle and the scene. Under various scenes, the changes in conversion factor with the solar zenith angle are different. When the solar zenith angle is small, the conversion factor is quite sensitive to the various scenes, its values can change from 2.54 to 5.3 for GMS satellite data. But under the larger solar zenith angle, the difference in value of the conversion factor for various scenes is very small. Under a certain solar zenith angle but different observation angles (observing zenith angle and azimuth),the value of the conversion factor is also changed. The deviation from mean value under a certain solar zenith angle is obviously large for larger solar zenith angle and ocean scene. The mean relative differences are about 5%–15% for ocean, 4.5%–10% for various land and $< 4\%$ for snow and cloud scenes.

The angular anisotropic correction is also made. The anisotropic reflectance factor estimated with the help of the radiative model is compared to the observed from Nimbus-7 Earth Radiation Budget Experiment. It is found that both are agreeable for ocean and cloud scenes and that there is some difference in forward scattering for scenes of land, desert and snow. The reasons for the difference are that the surface is regarded as isotropic in the model calculation and that the calculated values of anisotropic reflectance factor are for a certain solar zenith angle while the values estimated by Nimbus-7 are for a range of solar zenith angle. Due to insufficient anisotropic surface reflection data and too much computation time required in the calculation of anisotropic reflectance factor, the Nimbus-7 experiment data can be directly employed in some researches. However, the anisotropic reflectance factor estimated from Nimbus-7 experment is given only for 8 solar zenith angle ranges and for 56 bins in each range. It is insufficient for retrieval of broadband radiation fluxes or broadband planetary albedo. With radiative transfer modelling the anisotropic reflectance factor can be calculated for any solar zenith angle and for sufficient number of bins (such as 306 bins in this paper).

In further efforts, the model input data about surface reflexion should be improved. For this propose the anisotropic data published for various surface condition should be collected and some available compensatory measurements about surface anisotropic reflectance property should be made. With these data, the anisotropic model results in backward and forward scattering direction can be more accurate. This work (here in this paper) is also available for other satellite data. For example, using the Fengyun satellite spectral response function in-

stead of GMS spectral response function, the spectral and anisotropic corrections can also be obtained for Fengyun satellite data. Therefore, further work is to calculate and establish the dataset of the conversion and anisotropic factors for GMS and Fengyun satellite data.

The author gratefully acknowledge Prof. Dr. E. Raschke for his encouragement of this study and critically reading of the manuscript. I also acknowledge the valuable discussions with Dr. R. Stuhlmann and with colleagues in Institute of Geophysics and Meteorology, Cologne University.

REFERENCES

Cess, R. D. and G. L. Potter (1986), Narrow-and Broadband Satellite Measurements of Shortwave Radiation: Converaion Simulstion with a General Circulation Model, *J. Climate Appl. Meteor.* **25:** 1977–1984.

Cox, C. and W. Munk (1955), Some Problems in Optical Oceanography, *J. Mar. Res.*, **14:** 63.

Dirmhirn, I. and F. D. Eaton (1975), Some Characteristics of the Albedo of Snow, *J. Appl. Meteor.*, **14:** 275–370.

Frohlich, C. (1987), Variablity of the Solar " Constant" on Time Scales of Minutes to Years, *J. Geophys. Res.*, **92:** No. D1, 795–800.

GMS Users' Guide (1980), Meteorological Satellite Center, 3–235 Nakakiyoto, Kiyose, Tokyo, 180–04, Japan.

Hansen, J. E. (1971), Mutiple Scattering of Polarized Light in Planetary Atmosphere, Part 2, Sunlight Reflected by Terrestrical Water Clouds, *J. Atmos. Sci.*, **28:** 1400–1426.

Kerschgens, M., U. Pilz und E. Raschke (1978), A Modified Two-stream Approximation for Computation of the Solar Radiation Budget in a Cloudy Atmosphere, *Tellus*, **30:** 429–435.

Koepke, P. and K. T. Kriebel (1987), Improvements in the Shortwave Cloud-free Radiation Budget Accuracy, Part I: Numerical Study Including Surface Anisotropy, *J. Climate Appl. Meteor.*, **26:** 374–409.

Kriebel, K. T. (1978), Measured Spectral Bidirectional Reflection Properties of Vegetated Surfaces, *Appl. Opt.*, **17:** 253–259.

Kriebel, K. T. (1983), Results of METEOSAT–2 VIS– Channel Calibration, *Proc. Fourth METEOSAT Scientific User Meeting*, Clermont–Ferrand., ESOC.

McClatchey, R. A., H. J. Bolle and K. Ya. Kondratyev (1977), Report on the IAMAP Radiation Commission Working Group on a Standard Radiation Atmosphere, Seattle, Wash.

Potter, J. F. (1970), The Dalta Function Approximation in Radiative Transter Theory, *J. Atmos. Sci.*, **27:** 943–949.

Quenzel, H. and H. MUller (1978), Optical Property of Single Mie Partiles, Wiss. Mitteilung, Meteorologisches Institut, Universitat München, No. 34.

Raschke, E. (1971), Berechnungen des durch Mehrfachstreuung entstehenden Feldes solarer Strahlung in einem System Ozean–Atmospare, BMBW–FBW 71–20, Bereich Extraterrestische Physik der Universitat Bochum.

Raschke, E. (1972), Multiple Scattering Calculations of Sclar Radiation in an Atomsphere–Ocean System, *Beitr. Phys. Atmosph.*, **45:** No. 1, 1–19.

Shettle, E. P. and R. W. Fenn(1975), Model of the Atmospheric Aerosols and their optical properties, *Adv. Group for Aerospace Res.* and Dev. (AGARD), Conf. *Proc. 183 of Optical Propagation in the Atmosphere.*

Stuhlmann, R., P. Minnis and G. L. Smith (1985), Cloud Bidirectional Reflectance Function : a Comparison of Experimental and Theoretical Results, *Appl.,Opt.*, **24:** 396–401.

Stuhlmann, R. and E. Raschke (1987), Satellite Measurement of the Earth Radiation Budget: Sampling and Retrieval of Short Wave Exitance–A Sampling Study, *Beitr. Phys. Atmosph.*, **60:** No. 3, 393–410.

Stum, J., B. Pinty and D. Ramond (1985), A Parameterization of Broadband Conversion Factors for METEOSAT Visible Radiances, *J. Climate Appl. Meteor.*, **24:** 1377–1382.

Taylor. V. R. and L. L. Stowe (1984), Reflectance Characteristics of Uniform Earth and Cloud Surfaces Derived from NIMBUS–7 ERB, *J. Geoph. Res.*, **89:** 4987–4996.

Wiegner. W. (1985), Bestimmung der Strahlungsbilanz am Oberrand der Atmosphre ber der Sahara aus Satellitenmessungen, *Mitteilungen fur Geophysik und Meteorologie der Universitt zu Kln*,Heft 43.